The SIR Meta Distribution in Poisson Cellular Networks with Base Station Cooperation

Qimei Cui, *Senior Member, IEEE,* Xinlei Yu, Yuanjie Wang, and Martin Haenggi, *Fellow, IEEE*

***Abstract*—The meta distribution provides fine-grained information on the signal-to-interference ratio (SIR) compared to the SIR distribution at the typical user. This paper firstly derives the meta distribution of the SIR in heterogeneous cellular networks with downlink coordinated multipoint transmission/reception (CoMP), including joint transmission (JT), dynamic point blanking (DPB), and dynamic point selection/dynamic point blanking (DPS/DPB), for the general typical user and the worst-case user (the typical user located at the Voronoi vertex in a single-tier network). A more general scheme called JT-DPB, which is the combination of JT and DPB, is studied. The moments of the conditional success probability are derived for the calculation of the meta distribution and the mean local delay. An exact analytical expression, the beta approximation and simulation results of the meta distribution are provided. From the theoretical results, we gain insights on the benefits of different cooperation schemes and the impact of the number of cooperating base stations and other network parameters.**

***Index Terms*—Base station cooperation, CoMP, meta distribution, mean local delay, cellular network, HetNets, Poisson point process, stochastic geometry.**

I. Introduction

A. Motivation

With the increasing demand for data rate over cellular networks, the heterogeneous networks are deployed more and more densely [1]. In order to reduce the additional inter-cell interference caused by network densification and heterogeneity, coordinated multipoint transmission/reception (CoMP) is a key technology in cellular networks. Stochastic geometry provides unified mathematical tools to model and analyze wireless networks with randomly placed nodes, including cellular networks [2]. In order to comprehensively assess the benefits of CoMP, the meta distribution of the signal-to-interference ratio (SIR), a recently introduced performance metric [3], needs to be studied. The standard (mean) success probability defined as the complementary cumulative distribution function (CCDF) of the SIR of the typical user answers the questions "Given a SIR threshold[1] θ, what fraction of users in the whole network can achieve successful transmission on average?", while the meta distribution provides more fine-grained information for the individual links than the standard success probability and answers more detailed questions such as "What fraction of users in a cellular network achieve 90% link reliability given a SIR threshold θ?" [3].

Letting Φ denote the point process of base stations (BSs), the meta distribution is the CCDF of the conditional success probability

$$P_{\mathrm{s}}(\theta) \triangleq \mathbb{P}(\mathrm{SIR} > \theta \mid \Phi), \tag{1}$$

which is the CCDF of the SIR of the user at the origin given the point process Φ. The meta distribution is formally defined by [3] as

$$\bar{F}(\theta, x) \triangleq \bar{F}_{P_{\mathrm{s}}}(\theta, x) = \mathbb{P}(P_{\mathrm{s}}(\theta) > x), \quad x \in [0, 1]. \tag{2}$$

Since it is difficult, most likely impossible, to calculate the meta distribution directly from the definition in (2), we focus on the moments of $P_s(\theta)$. The b-th moment of $P_s(\theta)$ is denoted by

$$\begin{aligned} M_b(\theta) \triangleq \mathbb{E}(P_{\mathrm{s}}(\theta)^b) &= \int_0^1 x^b \mathrm{d}\bar{F}_{P_{\mathrm{s}}}(x) \\ &= \int_0^1 b x^{b-1} \bar{F}_{P_{\mathrm{s}}}(x) \mathrm{d}x, \quad b \in \mathbb{C}, \end{aligned} \tag{3}$$

and the standard success probability can be expressed as $p_{\mathrm{s}}(\theta) \equiv M_1(\theta)$, i.e., the first moment of the conditional success probability. The exact meta distribution can then be obtained by the Gil-Pelaez theorem [4] from the purely imaginary moments $M_{jt} = \mathbb{E}(P_{\mathrm{s}}(\theta)^{jt})$, $j \triangleq \sqrt{-1}$, $t \in \mathbb{R}^+$. It is noteworthy that the meta distribution is the distribution of the conditional success probability $P_s(\theta)$, while the standard success probability captures only the mean of $P_s(\theta)$.

B. Related Work

Due to the simple form of its probability generating functional (PGFL) [5, Theorem 4.9], the Poisson point process (PPP) is the most tractable model for the analysis of wireless networks based on stochastic geometry. Most of the prior works focus on the standard success (coverage) probability (M_1 in our notation) as the performance metric [6]–[9]. The standard success probability is the spatial average over the channel fading and the point process. This important value

Manuscript date November 13, 2017.

Qimei Cui and Xinlei Yu are with School of Information and Communication Engineering, Beijing University of Posts and Telecommunications, Beijing, 100876, China (e-mail: cuiqimei@bupt.edu.cn, xinleiyu@hotmail.com). Yuanjie Wang is with the State Key Laboratory of Railway Traffic Control and Safety, Beijing Jiaotong University, Beijing, 100044, China (e-mail: wang.yuanjie@outlook.com). Martin Haenggi is with the Dept. of Electrical Engineering, University of Notre Dame, IN, 46556, USA (e-mail: mhaenggi@nd.edu).

The work was supported in part by the National Nature Science Foundation of China Project under Grant 61471058, in part by the Hong Kong, Macao and Taiwan Science and Technology Cooperation Projects under Grant 2016YFE0122900, in part by the 111 Project of China under Grant B16006, and in part by the U.S. National Science Foundation under Grant CCF 1525904.

[1]In theory, the SIR threshold can be set arbitrarily. In practice, since different user services have different requirements of quality of services (QoS), the operator chooses the threshold according to different QoS requirements.

gives some basic information on the SIR performance of the network, but does not provide information on the distribution of the individual link reliability. In order to gain more fine-grained information for each individual link in the network, the meta distribution is formally defined in [3]. The b-th moment for $b \in \mathbb{C}$ of the conditional success probability for both Poisson bipolar networks and downlink cellular networks is derived for the calculation of the exact meta distribution. Besides, a simple approximation of the meta distribution is obtained by matching the first and second moment with a beta distribution, which provides an excellent match with the meta distribution. In [10], the meta distribution and mean local delay of the typical device-to-device (D2D) user and cellular downlink user are analyzed for the D2D communication underlaid Poisson downlink cellular networks in which the D2D users form a Poisson bipolar network. In [11], the meta distribution of the SIR is analyzed for both uplink and downlink cellular networks with fractional power control. [12] uses the signal-to-interference-plus-noise ratio (SINR) instead of the SIR to analyze the meta distribution of millimeter-wave D2D networks. Due to the unique features of millimeter-wave communication, a generalized beta distribution approximation related to the noise level is proposed to obtain a better fit for the meta distribution.

In the framework of 3GPP, downlink CoMP transmission is categorized as joint transmission (JT), dynamic point selection (DPS), dynamic point blanking (DPB), and coordinated scheduling/beamforming (CS/CB) [13], [14]. These cooperation techniques have been studied in prior work using stochastic geometry, but not in terms of the meta distribution.

With JT, the user receives multiple desired signals that are jointly transmitted on the same time-frequency resource by a subset of all BSs in the network. In [15], the authors use stochastic geometry to analyze JT for downlink heterogeneous cellular networks modeled as multiple tiers of independent PPPs. The general user and the user located at the cell-corner (the so-called worst-case user) are considered. In order to evaluate the performance, the standard success probability is derived under the assumption that the BSs have no channel state information (CSI). The case of full CSI is evaluated in terms of different performance metrics (diversity gain and power gain). [16], [17] analyze these performance metrics of both the general and worst-case users in heterogeneous cellular networks with spatiotemporal cooperation techniques including JT, base station silencing, and the Alamouti space-time code, and the decoding techniques including hybrid automatic repeat request (HARQ) and maximum ratio combining (MRC). [18] uses a single-tier Poisson cellular network model to analyze non-coherent JT in term of the SINR distribution and studies the effect of imperfect CSI and intra-cluster scheduling on non-coherent JT.

With DPS, the user receives a desired signal that is transmitted by the BS with the best instantaneous channel condition in a cooperation set. In [8], under the assumption that the SINR threshold is greater than 1 (0 dB), the standard success probability is analyzed using stochastic geometry for K-tier downlink heterogeneous Poisson cellular networks in which the serving BS can be selected from all BSs dynamically. With DPB, the BSs with dominant interference to the user in the cooperation set are silenced based on the average received power, where the average is taken over the fading. It is noteworthy that DPB is sometimes called inter-cell interference coordination (ICIC). [9] models BSs as a homogeneous PPP and provides explicit integral expressions for the success probability for cellular networks with ICIC. In order to obtain higher performance gains, DPS is usually combined with DPB, namely DPS/DPB. Currently, there is no analysis of DPS/DPB based on stochastic geometry in Poisson cellular networks.

There are very few works on the joint use of JT and DPB. It is mentioned in a 3GPP technical report [13], but it is only stated that DPS/DPB may be combined with JT, in which case multiple base stations can be selected for data transmission in the time-frequency resource. [19], [20] introduces a novel combined algorithm between JT and DPB (ICIC), but only Monte Carlo simulation results are provided. [21] proposes an adaptive method with the combination between JT and ICIC and focuses on the joint parameter optimization of JT and ICIC. A rigorous analysis for this combined scheme is still an open issue.

C. Contributions

In this paper, we focus on the meta distribution of the SIR in heterogeneous cellular networks with the downlink CoMP schemes including JT, DPB, and DPS/DPB. A more general scheme called JT-DPB, which is the combination of JT and DPB, is studied. We consider two types of typical users—the general user and the worst-case user. The general user corresponds to the general typical user, while the worst-case user is the typical user located at the Voronoi vertex in a single-tier network, i.e., the typical cell-corner user.

The contributions of the paper are:

- A more general scheme called JT-DPB is analyzed rigorously for the first time, with JT and DPB as special cases. We show the comparison of JT, DPB, and the combined JT-DPB scheme. Furthermore, we give the first rigorous analysis of DPS/DPB based on stochastic geometry.
- We derive the b-th moment of the conditional success probability for both types of users with the combined JT-DPB scheme. For DPS/DPB, the first moment (standard success probability) for the general user and the first and second moment for the worst-case user are derived.
- The mean local delay, which is the -1-st moment of the conditional success probability, is derived for both types of users with JT-DPB. The critical values of the phase transition from finite to infinite mean local delay are also obtained.
- We calculate the exact meta distribution for the worst-case user with JT-DPB and the beta distribution approximation of the exact meta distribution for almost all schemes and user types. We show that the beta approximation provides an accurate match for the exact meta distribution obtained by analysis and simulation. By the analysis of the meta distribution, we provide more fine-grained information of the link reliability for the study of CoMP.

- From the theoretical results, we gain insights on the benefits of different cooperation schemes and the impact of the number of cooperating base stations and other network parameters.

II. System Model

A. Cellular Network Model

We consider a K-tier PPP heterogeneous cellular network model where the BSs belonging to i-th tier are distributed in $\mathbb{R}^2$ according to a homogeneous PPP Φ_i with density λ_i and transmit power P_i, $i = 1, \ldots, K$. We focus on the typical user at the origin $(0,0) \in \mathbb{R}^2$. In order to study the downlink CoMP, we denote the cooperation set by $\mathcal{C} \subset \Phi$, where $\Phi \triangleq \bigcup_{i=1}^{K} \Phi_i$, i.e., BSs from all network tiers can cooperate. The typical user receives the same message that is transmitted synchronously by a subset of $\mathcal{C}$, which is denoted by $\mathcal{O} \subseteq \mathcal{C}$. Let n denote the size of $\mathcal{C}$ and m denote the size of $\mathcal{O}$, hence $m \leq n$. For JT, $\mathcal{O} = \mathcal{C}$, i.e., $m = n$. The received channel output at the typical user can be written as

$$\sum_{x \in \mathcal{O}} P_{\nu(x)}^{1/2} \|x\|^{-\alpha/2} h_x w_x X + \sum_{x \in \mathcal{C}^c} P_{\nu(x)}^{1/2} \|x\|^{-\alpha/2} h_x w_x X_x + N, \tag{4}$$

where the first sum is the desired signal from the cooperating BSs in subset $\mathcal{O}$, the second sum is the interference from the non-cooperating BSs, and N is additive white Gaussian noise, i.e., $N \sim \mathcal{N}_{\mathbb{C}}(0, \sigma^2)$; $\nu(x)$ denotes the index of the network tier of the BS located at x, i.e., $\nu(x) = i$ iff $x \in \Phi_i$; h_x denotes the Rayleigh fading between the typical user at the origin and the BS at x, $h_x \sim \mathcal{N}_{\mathbb{C}}(0,1)$ and h_x is i.i.d.; w_x is the precoder at BS x; $\alpha > 2$ is the path loss exponent; $\mathcal{C}^c = \Phi \backslash \mathcal{C}$ denotes the BSs that are not in the cooperation set; X denotes the channel input symbol transmitted by the BSs in $\mathcal{O}$, and X_x denotes the channel input symbol transmitted by the BS which is at $x \in \mathcal{C}^c$. We assume that X and X_x are i.i.d. uniform random variables with zero mean. Since the typical heterogeneous cellular networks are interference-limited and the noise has very limited effect on the success probability [8], [15], [22], we focus on the interference-limited regime, i.e., N is ignored.

B. General and Worst-case Users

Fig. 1 shows an illustration of two types of typical users—the general user and the worst-case user. For the general user, we focus on the typical user located at the origin in a K-tier heterogeneous cellular network, the cooperation set $\mathcal{C}$ consists of the n BSs with the strongest average received power for arbitrary $n \in \mathbb{Z}^+$, i.e.,

$$\mathcal{C} = \arg \max_{\{x_1, \ldots, x_n\} \subset \Phi} \sum_{i=1}^{n} \frac{P_{\nu(x_i)}}{\|x_i\|^{\alpha}}, \quad n \in \mathbb{Z}^+. \tag{5}$$

Prior research has demonstrated that CoMP can improve system spectral efficiency and, in particular, significantly enhance the cell-edge spectral efficiency [13], [23]. Hence, in order to study the cell-edge performance, in addition to the general user, we consider another type of users named the worst-case user as in [15], which is located at the Voronoi vertex in a single-tier network in $\mathbb{R}^2$ modeled by a homogeneous PPP Φ with density λ and transmit power P. A Voronoi vertex is a location at equal distance from three BSs. In this case, it is natural that we restrict the size of the cooperation set to $n \in \{1, 2, 3\}$ since the user has three equidistant BSs. Without loss of generality, we assume a Voronoi vertex to be located at $(0,0)$, i.e., we condition on Φ having a Voronoi vertex at $(0,0)$, and we place a user at this location. Hence the cooperation set $\mathcal{C}$ of this user is the subset of three BSs that are all closest to the origin. Denoting the location of the i-th closest BS to the origin by x_i, the cooperation set is

$$\mathcal{C} \subseteq \{x_1, x_2, x_3\}, \tag{6}$$

with $\|x_1\| = \|x_2\| = \|x_3\| = D$.

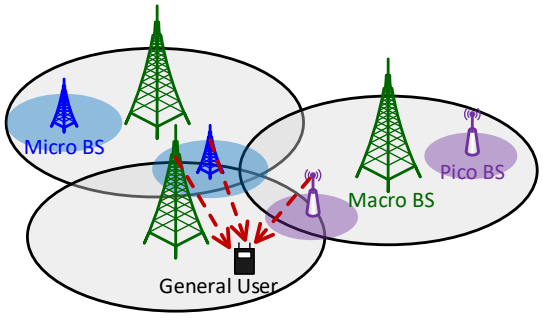

(a) General User

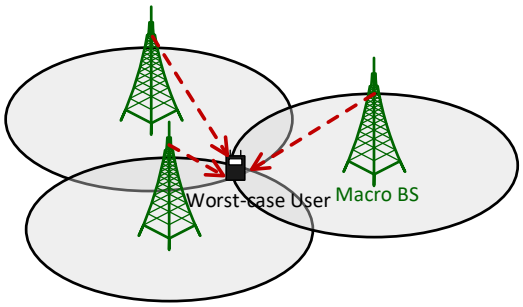

(b) Worst-case User

Fig. 1. Two types of typical users—general user and worst-case user.

III. Meta Distribution for JT-DPB

A. SIR Model

With JT, all the BSs in a cooperation set jointly transmit the same message to a target user on the same time-frequency resource, i.e., all the BSs in a cooperation set are serving BSs for the target user, i.e., $m = n$. With DPB, in a cooperating set, the user receives a message that is transmitted by the BS with strongest average received power and the other BSs in the cooperation set are silenced, i.e., $m = 1$. Given a user, for both CoMP schemes, the serving BSs are uniquely determined by the transmit power, distance, and m. The only difference between JT and DPB is m. Hence, we consider a more general scheme, which is the combination of JT and DPB, called JT-DPB. In this scheme, JT is the special case where $m = n$, and DPB is the special case where $m = 1$. The cases where $m = 2, 3, \ldots, n-1$ are combined JT-DPB schemes.

In the framework of 3GPP LTE, JT is categorized into coherent and non-coherent JT [13]. The coherence[2] of JT refers to the ability to form precoders that exploit the phase and potential amplitude relations between channels associated with different serving BSs [28].

In the case of coherent JT it is assumed that the network has detailed CSI of the serving links from the BSs in the cooperation set to the same single user [29]. Based on the CSI shared among all cooperating BSs, the transmitted signals from different BSs are jointly precoded with prior phase alignment and tight synchronization across BSs to achieve coherent combining at the served user. There is currently no support in the 3GPP LTE specifications for the user to report this kind of detailed CSI for multiple BSs in the cooperation set, and thus there is currently no explicit support for coherent JT.

In contrast, for non-coherent JT, a BS in the cooperation set only knows its own CSI and cannot get the CSI from other cooperating BSs. The transmitted signals from each serving BS are individually precoded based on the CSI of that specific serving link, therefore a phase mismatch exists between the multiple useful signals at the served user. Non-coherent JT is supported in 3GPP LTE specification Release 11. In this section, we consider a special case of non-coherent JT, in which the BSs have no CSI and the transmitted signals from each serving BS are without precoder, i.e., $w_x = 1$, and blind demodulation is used at the user [15]–[17], [30], [31]. Throughout this section, JT refers to this scheme.

The SIR of the general user with JT-DPB is given by

$$\mathrm{SIR}_{\mathrm{g}}^{\text{JT-DPB}} = \frac{\left|\sum_{x\in\mathcal{O}} P_{\nu(x)}^{1/2}\|x\|^{-\alpha/2}h_x\right|^2}{\sum_{x\in\mathcal{C}^c} P_{\nu(x)}\|x\|^{-\alpha}|h_x|^2}. \tag{7}$$

For every $i = 1,\ldots,K$, let $\Xi_i = \{\|x\|^\alpha / P_i \,, x \in \Phi_i\}$. By the mapping theorem [5, Theorem 2.34] and the superposition property [5, Section 2.5] of the PPP, $\Xi = \bigcup_{i=1}^K \Xi_i$ is a non-homogeneous PPP on $\mathbb{R}^+$ with intensity function

$$\lambda(x) = \sum_{i=1}^{K} \lambda_i \pi \delta P_i^\delta x^{\delta-1}, \quad x \in \mathbb{R}^+, \tag{8}$$

where $\delta = 2/\alpha$. We sort the elements of Ξ in ascending order, such that $\|x_1\|^\alpha / P_{\nu(x_1)} \le \|x_2\|^\alpha / P_{\nu(x_2)} \le \|x_3\|^\alpha / P_{\nu(x_3)} \le \cdots$, define $\gamma_k = \|x_k\|^\alpha / P_{\nu(x_k)}$ as the k-th element in the ordered set, and name γ_k the normalized path loss. The SIR in (7) can be re-written as

$$\mathrm{SIR}_{\mathrm{g}}^{\text{JT-DPB}} = \frac{\left|\sum_{k=1}^{m} h_{x_k}\gamma_k^{-1/2}\right|^2}{\sum_{k=n+1}^{\infty}\gamma_k^{-1}g_k}, \tag{9}$$

where $g_k = |h_{x_k}|^2$ and $m \le n$.

[2]In traditional communication theory, coherence refers to the ability to track the phase of the signal, while in 3GPP LTE, it has a more general meaning, including joint precoding [23]–[27].

Similarly, for $n = 1, 2, 3$, the SIR of the worst-case user with JT-DPB is

$$\begin{aligned}\mathrm{SIR}_{\mathrm{w}}^{\text{JT-DPB}} &= \frac{P\left|\sum_{x\in\mathcal{O}}\|x\|^{-\alpha/2}h_x\right|^2}{\sum_{x\in\Phi\setminus\mathcal{C}} P\|x\|^{-\alpha}|h_x|^2} = \frac{\left|\sum_{k=1}^{m}\|x_k\|^{-\alpha/2}h_{x_k}\right|^2}{\sum_{k=n+1}^{\infty}\|x_k\|^{-\alpha}g_k} \\ &\overset{(a)}{=} \frac{\left|\sum_{k=1}^{m} D^{-\alpha/2}h_{x_k}\right|^2}{\sum_{k=n+1}^{3} D^{-\alpha}g_k + \sum_{k=4}^{\infty}\|x_k\|^{-\alpha}g_k},\end{aligned} \tag{10}$$

where $m \le n$, and (a) follows since the distances between the target user and its three nearest BSs are equal, i.e., $\|x_1\| = \|x_2\| = \|x_3\| = D$.

B. Moments

Lemma 1 (Conditional success probability for the general user with JT-DPB) *The conditional success probability for the general user with JT-DPB is given by*

$$P_{\mathrm{s}}(\theta) = \prod_{k=n+1}^{\infty} \frac{1}{1+\theta G_m \gamma_k^{-1}}, \tag{11}$$

where $G_m \triangleq 1/\sum_{i=1}^m \gamma_i^{-1}$ *is the* parallel connection *(in the sense of parallel resistors) of the normalized path loss values* $\gamma_1,\ldots,\gamma_m$.

Proof: According to the assumption of Rayleigh fading and the independence of the fading coefficients $h_{x_1}, h_{x_2}, \ldots, h_{x_m}$, $\left|\sum_{k=1}^m \gamma_k^{-1/2}h_{x_k}\right|^2$ is exponentially distributed with mean $\sum_{k=1}^m \gamma_k^{-1}$. Letting $I = \sum_{k=n+1}^{\infty} g_k\gamma_k^{-1}$, the conditional success probability for the general user with JT-DPB can be derived as

$$\begin{aligned}P_{\mathrm{s}}(\theta) &= \mathbb{P}(\mathrm{SIR}_{\mathrm{g}}^{\text{JT-DPB}} > \theta \mid \Xi) \\ &= \mathbb{P}\left(\left|\sum_{k=1}^{m} h_{x_k}\gamma_k^{-1/2}\right|^2 > \theta I \mid \Xi\right) \\ &= \mathbb{E}\left(\exp\left(-\frac{\theta I}{\sum_{k=1}^m \gamma_k^{-1}}\right) \mid \Xi\right) \\ &= \mathbb{E}\left(\exp\left(-\frac{\theta}{\sum_{k=1}^m \gamma_k^{-1}}\sum_{k=n+1}^{\infty} g_k\gamma_k^{-1}\right) \mid \Xi\right) \\ &= \mathbb{E}\left(\prod_{k=n+1}^{\infty}\exp\left(-\frac{\theta}{\sum_{i=1}^m \gamma_i^{-1}}g_k\gamma_k^{-1}\right) \mid \Xi\right) \\ &\overset{(a)}{=} \prod_{k=n+1}^{\infty}\frac{1}{1+\frac{\theta}{\sum_{i=1}^m \gamma_i^{-1}}\gamma_k^{-1}},\end{aligned}$$

where (a) follows since $g_k = |h_{x_k}|^2$ are i.i.d. exponential with unit mean. ∎

Theorem 1 (Moments of $P_{\mathrm{s}}(\theta)$ for the general user with JT-DPB) *For every $n \ge 1$, the b-th moment M_b of the*

conditional success probability $P_{\rm s}(\theta)$ for the general user in downlink cellular networks with JT-DPB is

$$M_b = \int\limits_{\substack{0<u_1<\cdots\\ \cdots<u_n<\infty}} \exp\left(-u_n\ {}_2F_1\left(b,-\delta;1-\delta;\frac{-\theta}{\sum\limits_{i=1}^{m}\left(\frac{u_n}{u_i}\right)^{\frac{1}{\delta}}}\right)\right)\mathrm{d}\mathbf{u}, \tag{12}$$

where $\delta = 2/\alpha$, and ${}_2F_1(\cdot)$ is the Gaussian hypergeometric function.

Proof: The joint probability density function of $\boldsymbol{\gamma} = (\gamma_1, \gamma_2, \ldots, \gamma_n)$ is given by [15, Eqn. (37)], i.e., for $0 < \gamma_1 < \cdots < \gamma_n$,

$$f_{\boldsymbol{\gamma}}(\boldsymbol{r}) = \left(\pi\delta\sum_{i=1}^{K}\lambda_i P_i^{\delta}\right)^n \exp\left(-\pi\sum_{i=1}^{K}\lambda_i P_i^{\delta} r_n^{\delta}\right)\prod_{i=1}^{n} r_i^{\delta-1}. \tag{13}$$

Using the PGFL of the non-homogeneous PPP Ξ, M_b follows as

$$\begin{aligned} M_b &= \mathbb{E}\big(P_{\rm s}(\theta)^b\big) = \mathbb{E}\Big(\prod_{k=n+1}^{\infty}\left(\frac{1}{1+\theta G_m\gamma_k^{-1}}\right)^b\Big) \\ &= \int\limits_{\substack{0<r_1<\cdots\\ \cdots<r_n<\infty}} \exp\left(-\int_{r_n}^{\infty}\left(1-\frac{1}{\left(1+\frac{\theta x^{-1}}{\sum\limits_{i=1}^{m} r_i^{-1}}\right)^b}\right)\lambda(x)dx\right) f_{\boldsymbol{\gamma}}(\boldsymbol{r})\mathrm{d}\boldsymbol{r}, \end{aligned} \tag{14}$$

where $\lambda(x)$ is given in (8). Letting

$$\mathcal{L}_b(s) = \exp\left(-\int_{r_n}^{\infty}\left(1-\frac{1}{(1+sx^{-1})^b}\right)\lambda(x)\mathrm{d}x\right),$$

(14) can be written as

$$M_b = \int\limits_{\substack{0<r_1<\cdots\\ \cdots<r_n<\infty}} \mathcal{L}_b\left(\frac{\theta}{\sum_{i=1}^{m} r_i^{-1}}\right) f_{\boldsymbol{\gamma}}(\boldsymbol{r})\mathrm{d}\boldsymbol{r}. \tag{15}$$

Using the Gaussian hypergeometric function ${}_2F_1(\cdot)$, $\mathcal{L}_b(s)$ can be re-written as

$$\begin{aligned} \mathcal{L}_b(s) &= \exp\left(-\int_{r_n}^{\infty}\left(1-\frac{1}{(1+sx^{-1})^b}\right)\lambda(x)\mathrm{d}x\right) \\ &= \exp\left(-\pi\delta\sum_{i=1}^{K}\lambda_i P_i^{\delta}\cdot\int_{r_n}^{\infty}\left(1-\frac{1}{(1+sx^{-1})^b}\right)x^{\delta-1}\mathrm{d}x\right) \\ &= \exp\left(-\pi r_n^{\delta}\sum_{i=1}^{K}\lambda_i P_i^{\delta}\left({}_2F_1\left(b,-\delta;1-\delta;-\frac{s}{r_n}\right)-1\right)\right). \end{aligned} \tag{16}$$

Substituting (16) and (13) into (15), the b-th moment can be written as

$$\begin{aligned} M_b = \int\limits_{\substack{0<r_1<\cdots\\ \cdots<r_n<\infty}} &(\delta q)^n\prod_{i=1}^{n} r_i^{\delta-1} \\ &\cdot\exp\left(-qr_n^{\delta}{}_2F_1\left(b,-\delta;1-\delta;\frac{-\theta}{r_n\sum\limits_{i=1}^{m} r_i^{-1}}\right)\right)\mathrm{d}\boldsymbol{r}, \end{aligned} \tag{17}$$

where $q = \pi\sum_{i=1}^{K}\lambda_i P_i^{\delta}$. By changing the variable of this integration, i.e., letting $u_i = qr_i^{\delta}$, (12) follows. ∎

Lemma 2 (Conditional success probability for the worst–case user with JT-DPB) *For $n = 1, 2, 3$, the conditional success probability for the worst-case user with JT-DPB is given by*

$$P_{\rm s}(\theta) = \left(\frac{1}{1+\theta G_m D^{-\alpha}}\right)^{3-n}\prod_{k=4}^{\infty}\frac{1}{1+\theta G_m\|x_k\|^{-\alpha}}, \tag{18}$$

where $G_m = \frac{1}{mD^{-\alpha}}$.

Proof: According to the assumption of independent Rayleigh fading, $\left|\sum_{k=1}^{m} D^{-\alpha/2}h_{x_k}\right|^2$ is exponentially distributed with mean $mD^{-\alpha}$. The conditional success probability of the worst-case user is derived as

$$\begin{aligned} P_{\rm s}(\theta) &= \mathbb{P}(\mathrm{SIR}_{\rm w}^{\text{JT-DPB}} > \theta \mid \Phi) \\ &= \mathbb{P}\left(\left|\sum_{k=1}^{m} D^{-\alpha/2}h_{x_k}\right|^2 > \theta I \mid \Phi\right) \\ &= \mathbb{E}\left(\exp\left(-\frac{\theta I}{mD^{-\alpha}}\right)\mid\Phi\right) \\ &= \mathbb{E}\left(\exp\left(-\frac{\theta\Big(\sum\limits_{k=n+1}^{3} D^{-\alpha}g_k + \sum\limits_{k=4}^{\infty}\|x_k\|^{-\alpha}g_k\Big)}{mD^{-\alpha}}\right)\mid\Phi\right) \\ &= \mathbb{E}\Big(\prod_{k=n+1}^{3}\exp\left(-\frac{\theta g_k}{m}\right)\cdot\prod_{k=4}^{\infty}\exp\left(-\frac{\theta\|x_k\|^{-\alpha}g_k}{mD^{-\alpha}}\right)\mid\Phi\Big) \\ &\overset{(a)}{=} \left(\frac{1}{1+\frac{\theta}{m}}\right)^{3-n}\prod_{k=4}^{\infty}\frac{1}{1+\frac{\theta}{mD^{-\alpha}}\|x_k\|^{-\alpha}}, \end{aligned}$$

where (a) follows since $g_k = |h_{x_k}|^2$ is exponentially distributed with unit mean. ∎

Theorem 2 (Moments of $P_{\rm s}(\theta)$ for the worst-case user with JT-DPB) *For $n = 1, 2, 3$, the b-th moment M_b of the conditional success probability $P_{\rm s}(\theta)$ for the worst-case user in downlink cellular networks with JT-DPB is given by*

$$M_b = \int_0^{\infty} u\left(1+\frac{\theta}{m}\right)^{(n-3)b} \exp\left(-u\ {}_2F_1\left(b,-\delta;1-\delta;-\frac{\theta}{m}\right)\right)\mathrm{d}u, \tag{19}$$

where $\delta = 2/\alpha$.

When $b \in \mathbb{N}$, (19) *can be simplified to*

$$M_b = \frac{\left(1+\frac{\theta}{m}\right)^{(n-3)b}}{\left({}_2F_1(b,-\delta;1-\delta;-\frac{\theta}{m})\right)^2}. \tag{20}$$

Proof: The probability density function of the common distance D is [15, Eqn. (41)]

$$f_D(r) = 2\pi^2\lambda^2 r^3 e^{-\lambda\pi r^2}, \quad r \geq 0. \tag{21}$$

The b-th moments of $P_{\rm s}(\theta)$ are derived as

$$
\begin{aligned}
M_b &= \mathbb{E}\big(P_{\rm s}(\theta)^b\big) \\
&= \mathbb{E}\Bigg(\big(1+\theta G_m D^{-\alpha}\big)^{(n-3)b}\prod_{k=4}^{\infty}\left(\frac{1}{1+\theta G_m\|x_k\|^{-\alpha}}\right)^b\Bigg) \\
&\overset{(a)}{=} \mathbb{E}_D\Bigg(\left(1+\frac{\theta}{m}\right)^{(n-3)b} \\
&\quad\cdot\exp\left(-\int_D^{\infty}\left(1-\frac{1}{\big(1+\frac{\theta}{mD^{-\alpha}}x^{-\alpha}\big)^b}\right)2\pi\lambda x dx\right)\Bigg) \\
&= \int_0^{\infty}\left(1+\frac{\theta}{m}\right)^{(n-3)b} \\
&\quad\exp\left(-\int_r^{\infty}\left(1-\frac{1}{\big(1+\frac{\theta}{mr^{-\alpha}}x^{-\alpha}\big)^b}\right)2\pi\lambda x dx\right) f_D(r)\mathrm{d}r \\
&\overset{(b)}{=} \int_0^{\infty} 2\pi^2\lambda^2 r^3 e^{-\pi\lambda r^2}\left(1+\frac{\theta}{m}\right)^{(n-3)b} \\
&\quad\cdot\exp\left(-\pi\lambda r^2\left(-1+{}_2F_1\left(b,-\delta;1-\delta;-\frac{\theta}{m}\right)\right)\right)\mathrm{d}r \\
&= \int_0^{\infty} 2\pi^2\lambda^2 r^3\left(1+\frac{\theta}{m}\right)^{(n-3)b} \\
&\quad\cdot\exp\left(-\pi\lambda r^2\ {}_2F_1\left(b,-\delta;1-\delta;-\frac{\theta}{m}\right)\right)\mathrm{d}r, \qquad (22)
\end{aligned}
$$

where (a) follows from the PGFL of the homogeneous PPP Φ and (b) is derived by using the Gaussian hypergeometric function ${}_2F_1(\cdot)$. By the substitution $u=\pi\lambda r^2$, the result in (19) is obtained.

If $b\in\mathbb{N}$, then $\forall\theta>0$, ${}_2F_1(b,-\delta;1-\delta;-\theta/m)>0$. By using integration by parts, (19) can be written as

$$M_b=\frac{\big(1+\frac{\theta}{m}\big)^{(n-3)b}}{\big({}_2F_1(b,-\delta;1-\delta;-\frac{\theta}{m})\big)^2}.$$

■

Remark 1: Notice that (20) is the joint probability of b successful transmissions.

Remark 2: It is noteworthy in (12) and (19) that M_b for both the general user and the worst-case user with JT-DPB are independent of the transmit power P_i and the density λ_i of tier i in interference-limited heterogeneous networks. For M_1, this observation was made in [15, Remark 1] for JT and [8, Eqn. (3)] for non-CoMP.

Fig. 2 and Fig. 3 show the standard success probability $p_{\rm s}\equiv M_1$ and the variance of the conditional success probability for both types of users for non-coherent JT and DPB respectively. M_1 shown in Fig. 2(a) has been derived in [15], and M_1 for the general user with DPB shown in Fig. 3(a) corresponds to the result in [9]. Moreover, Fig. 4 compares these results of the combined scheme JT-DPB ($1<m<n$), non-coherent JT ($m=n$), and DPB ($m=1$).

Remark 3: It is remarkable that the (maximum) variance increases when n increases, as shown in Fig. 2(b), Fig. 3(b), and Fig. 4(b).

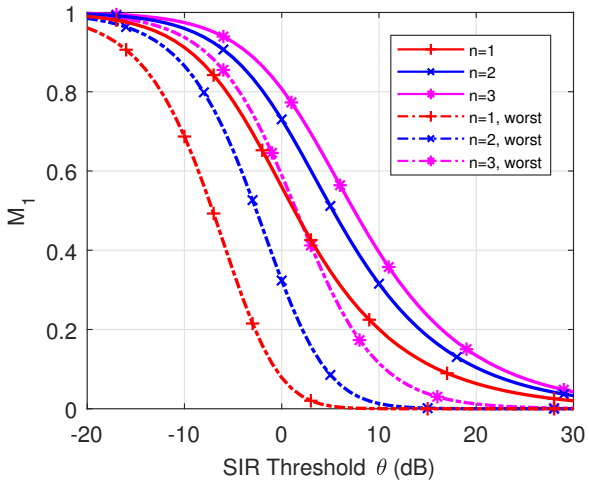

(a) M_1

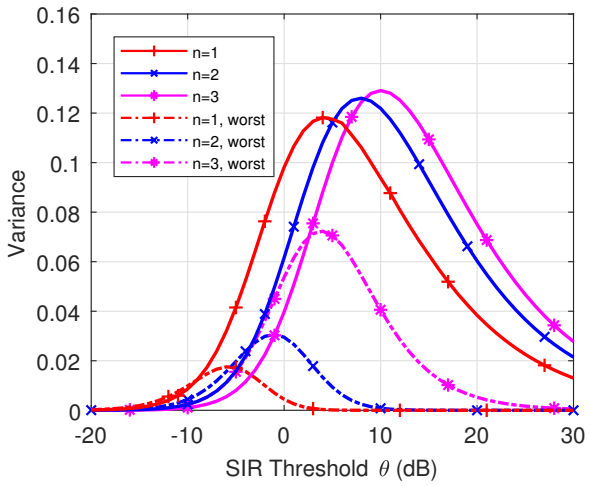

(b) Variance $M_2-M_1^2$

Fig. 2. M_1 and the variance (i.e. $M_2-M_1^2$) of $P_{\rm s}(\theta)$ for non-coherent JT where $n=m=1,2,3$, and $\alpha=4$.

C. Mean Local Delay M_{-1}

For a certain wireless link, the local delay, denoted by L, is the number of transmission attempts until the first success if the transmitter is allowed to keep transmitting packets [32]. Thus, the mean local delay can be expressed as $\mathbb{E}(L)=\mathbb{E}(\mathbb{E}(L\mid\Phi))$, where the inner expectation is over the fading and the outer expectation is over the point process Φ. Under the assumption that every transmission success event is conditionally independent given Φ[3], L is geometrically distributed with conditional success probability $P_{\rm s}$ conditioned on Φ, i.e.,

$$\mathbb{P}(L=k\mid\Phi)=(1-P_{\rm s})^{k-1}P_{\rm s},\quad k=1,\,2,\,3,\ldots. \qquad (23)$$

Hence, we have

$$\mathbb{E}(L)=\mathbb{E}(\mathbb{E}(L\mid\Phi))=\mathbb{E}\Big(\frac{1}{P_{\rm s}}\Big)=M_{-1}, \qquad (24)$$

i.e., the mean local delay is the -1-st moment of the conditional success probability, which is denoted by M_{-1}. In

[3]The conditional independence follows from the independence of the fading random variables from one transmission to the next.

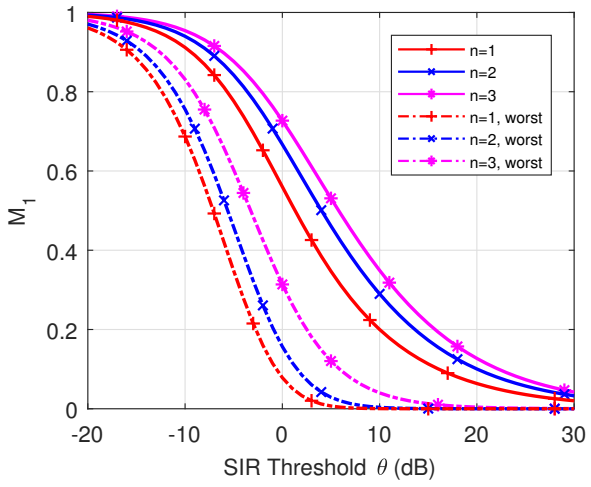

(a) M_1

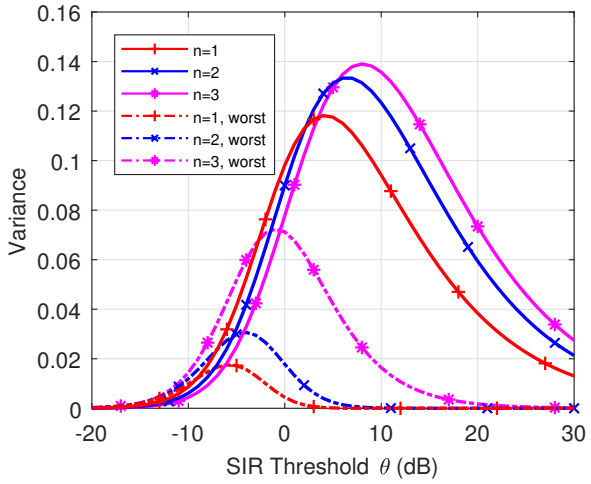

(b) Variance $M_2 - M_1^2$

Fig. 3. M_1 and the variance (i.e. $M_2 - M_1^2$) of $P_{\rm s}(\theta)$ for DPB where $m = 1$, $n = 1, 2, 3$, and $\alpha = 4$.

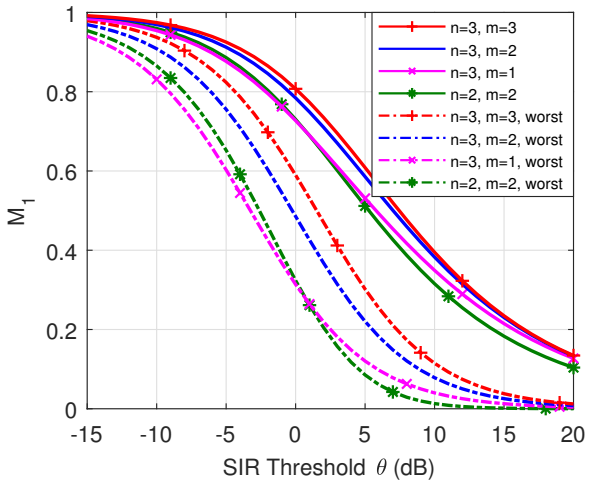

(a) M_1

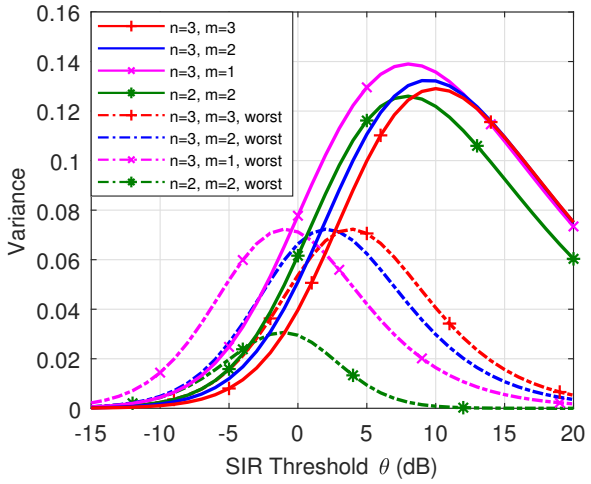

(b) Variance $M_2 - M_1^2$

Fig. 4. Comparison of M_1 and the variance (i.e. $M_2 - M_1^2$) of $P_{\rm s}(\theta)$ for non-coherent JT ($m = n$), DPB ($m = 1$), and the combined scheme JT-DPB ($1 < m < n$), where $\alpha = 4$.

downlink Poisson cellular networks, the mean local delay shows a phase transition at the critical value $\theta_{\rm critical}$, which means that as the SIR threshold θ reaches $\theta_{\rm critical}$, the mean local delay will jump from being finite to infinite [3], [10], [33]. An infinite mean local delay means that the fraction of links suffering from high delays is non-negligible. Put differently, the distribution of the local delay has a heavy tail.

Corollary 1 (Mean local delay for the general user with JT-DPB) *The mean local delay M_{-1} for the general user with JT-DPB is given by*

$$M_{-1} = \int\limits_{\substack{0<u_1<\cdots \\ \cdots<u_n<\infty}} \exp\left(-u_n + \frac{\theta u_n}{(1/\delta - 1)\sum_{i=1}^{m} \left(u_n/u_i\right)^{1/\delta}}\right) \mathrm{d}\mathbf{u}, \quad \theta < \theta_{\rm critical}, \tag{25}$$

where $\theta_{\rm critical} = (1/\delta - 1)m$.

Proof: By substituting $b = -1$ in (12), M_{-1} is given by

$$\begin{aligned} M_{-1} &= \int\limits_{\substack{0<u_1<\cdots \\ \cdots<u_n<\infty}} \exp\left(-u_n \; {}_2F_1\left(-1, -\delta; 1-\delta; \frac{-\theta}{\sum_{i=1}^{m} \left(\frac{u_n}{u_i}\right)^{\frac{1}{\delta}}}\right)\right) \mathrm{d}\mathbf{u} \\ &\overset{(a)}{=} \int\limits_{\substack{0<u_1<\cdots \\ \cdots<u_n<\infty}} \exp\left(-u_n + \frac{\theta u_n}{(1/\delta - 1)\sum_{i=1}^{m} \left(\frac{u_n}{u_i}\right)^{1/\delta}}\right) \mathrm{d}\mathbf{u}, \end{aligned}$$

where (a) follows since ${}_2F_1(-1, a; c; z) \equiv 1 - az/c$.

In fact, $\theta < \theta_{\rm critical}$ is the convergence condition of the improper integral expression M_{-1}. For the general user, if the improper integral expression M_{-1} is convergent, then for every

$$(u_1, u_2, \ldots, u_n) \in \{(u_1, u_2, \ldots, u_n) \in \mathbb{R}^n : 0 < u_1 < u_2 < \cdots < u_n\},$$

we have

$$-u_n + \frac{\theta u_n}{(1/\delta - 1)\sum_{i=1}^{m} \left(\frac{u_n}{u_i}\right)^{1/\delta}} < 0,$$

and thus

$$\sum_{i=1}^{m} \left(\frac{u_n}{u_i}\right)^{1/\delta} > \frac{\theta}{1/\delta - 1}.$$

Since $0 < u_1 < u_2 < \cdots < u_n$ and $m \leq n$, we have

$$\inf \sum_{i=1}^{m} \left(\frac{u_n}{u_i}\right)^{1/\delta} = m.$$

Hence $m > \frac{\theta}{1/\delta - 1}$. Consequently, $\theta_{\text{critical}} = (1/\delta - 1)m$. ■

Remark 4: For $n = m = 1$, i.e., the message is transmitted by only one BS without cooperation, (25) can be simplified to the closed-form expression

$$\begin{aligned} M_{-1} &= \int_0^{\infty} \exp\left(- u_1 + \frac{\theta u_1}{1/\delta - 1}\right) \mathrm{d}u_1 \\ &= \frac{1-\delta}{1-\delta(1+\theta)}, \qquad \theta < 1/\delta - 1, \end{aligned} \tag{26}$$

which is in line with the result in [3, Eqn. (24)].

Corollary 2 (Mean local delay for the worst-case user with JT-DPB) *For the worst-case user, the mean local delay M_{-1} for $n = 1, 2, 3$ with JT-DPB is given by*

$$M_{-1} = \frac{\left(1 + \frac{\theta}{m}\right)^{3-n}}{\left(1 - \frac{\theta}{(1/\delta - 1)m}\right)^2}, \quad \theta < \theta_{\text{critical}}, \tag{27}$$

where $\theta_{\text{critical}} = (1/\delta - 1)m$.

Proof: By substituting $b = -1$ in (19) and using ${}_2F_1(-1, a; c; z) \equiv 1 - az/c$, M_{-1} is given by

$$\begin{aligned} &M_{-1} \\ &= \int_0^{\infty} u \left(1 + \frac{\theta}{m}\right)^{3-n} \exp\left(-u\left(1 - \frac{\theta}{(1/\delta - 1)\, m}\right)\right) \mathrm{d}u \\ &= \begin{cases} \dfrac{\left(1 + \frac{\theta}{m}\right)^{3-n}}{\left(1 - \frac{\theta}{(1/\delta - 1)m}\right)^2}, & \theta < (1/\delta - 1)m \\ \infty, & \theta \geq (1/\delta - 1)m, \end{cases} \end{aligned}$$

and the critical value of θ is $\theta_{\text{critical}} = (1/\delta - 1)m$. ■

Fig. 5 shows the mean local delay for non-coherent JT and DPB for the general user and the worst-case user with $n = 1, 2, 3$ respectively, and the critical value of phase transition can be observed. For both general and worst-case users with non-coherent JT, the phase transitions occur at $\theta = 1, 2, 3$ (not in dB) for $n = 1, 2, 3$ respectively. In contrast, for DPB, the phase transition occurs at $\theta = 1$ (not in dB) for all users and all n.

Remark 5: The mean local delay of the worst-case user is larger than that of the general user. As the size of cooperation set n increases, the mean local delay of the worst-case user and the general user get closer, as shown in Fig. 5.

Remark 6: Interestingly, the critical value does not depend on the number of silenced BSs, i.e., only the number of jointly transmitting BSs m matters, and θ_{critical} increases linearly with m.

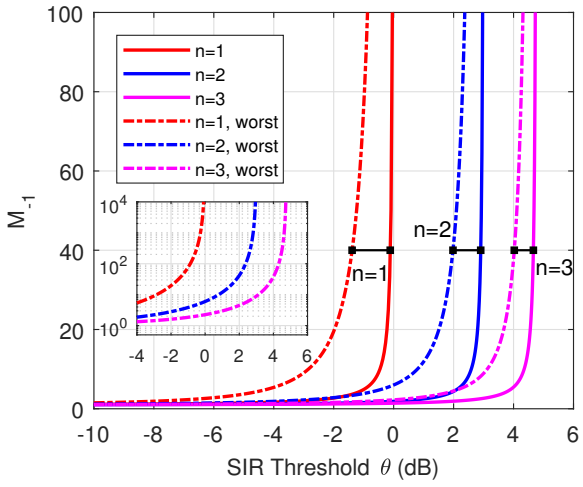

(a) non-coherent JT

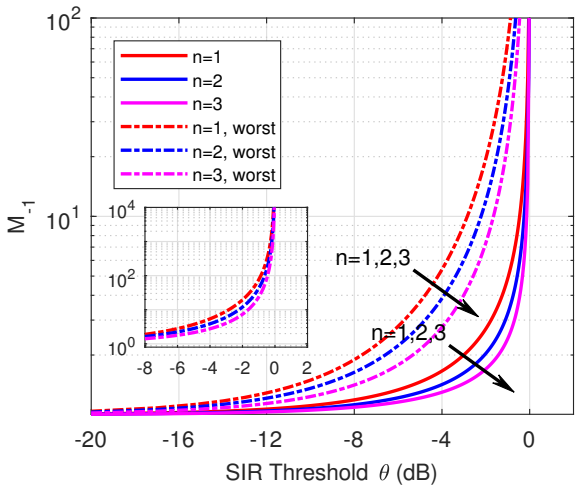

(b) DPB

Fig. 5. The mean local delay M_{-1} for the general and worst-case users for non-coherent JT and DPB, where $n = 1, 2, 3$, and $\alpha = 4$. The phase transitions can be observed in the figures.

D. Meta Distribution and its Beta Approximation

As mentioned earlier, the exact meta distribution can be obtained by the Gil-Pelaez theorem [4] from the purely imaginary moments $M_{jt} = \mathbb{E}(P_{\text{s}}(\theta)^{jt})$, $j \triangleq \sqrt{-1}$, $t \in \mathbb{R}^+$, as [3]

$$\bar{F}_{P_{\text{s}}}(x) = \frac{1}{2} + \frac{1}{\pi} \int_0^{\infty} \frac{\mathrm{Im}\left[e^{-jt \log x} M_{jt}\right]}{t} \mathrm{d}t. \tag{28}$$

This formula together with the moments in Theorem 1 and Theorem 2 show that the entire meta distribution for JT-DPB does not depend on the transmit powers and densities of each tier.

The numerical calculation of the exact meta distribution according to (28) is tedious. Alternatively, it is often sufficient to approximate the meta distribution by matching its first and second moment to the beta distribution, resulting in an excellent match. For cellular networks without CoMP, the excellent match between the meta distribution and the beta distribution has been confirmed in [3]. The beta distribution is a two-parameter continuous distribution supported on $[0, 1]$ and thus a natural candidate to approximate the distribution of

a conditional probability. Its CDF is given by the regularized incomplete beta function with shape parameters $a, b > 0$, i.e.,

$$I_x(a,b) = \frac{\int_0^x t^{a-1}(1-t)^{b-1}\mathrm{d}t}{B(a,b)}, \tag{29}$$

where $B(a,b)$ is the beta function. By matching first and second moments with M_1 and M_2, we obtain the approximated meta distribution

$$\bar{F}_{P_s}(x) \approx 1 - I_x\Big(\frac{M_1\beta}{1-M_1}, \beta\Big), \tag{30}$$

where

$$\beta = \frac{(M_1 - M_2)(1-M_1)}{M_2 - M_1^2}. \tag{31}$$

Furthermore, system-level simulations are carried out for comparison. Throughout the simulations in this section, since the entire meta distribution for JT-DPB is independent of the number of network tiers and their respective transmit powers and densities according to Theorem 1 and Theorem 2, without loss of generality, we focus on the case of a single-tier network, and P and λ can be set arbitrarily. Specifically, we produce 10000 PPP realizations, and then produce 1000 realizations of the Rayleigh fading random variables for each PPP realization. Next, we calculate the SIR of the target users and obtain the simulation results of the success probability, variance, and meta distribution over the 10000×1000 data points. The simulation parameters are: size of cooperation set $n = 1, 2, 3$, path loss exponent $\alpha = 4$, transmit power $P = 1$, density $\lambda = 1$, and simulation region $[-30, 30]^2$. In terms of the average number of BSs, there are about 3600 BSs in a simulation region, which is certainly sufficient.

Fig. 6(a) shows the meta distribution with non-coherent JT. For the general user, we confirm the accuracy of the beta distribution approximations by comparing the approximations with simulation results. For the worst-case user, the exact meta distribution can be calculated by using the Gil-Pelaez theorem. We calculate the exact meta distribution compared with its beta distribution approximation. Fig. 6(b) also shows these results for DPB. Fig. 7 compares the beta distribution approximation among the combined scheme JT-DPB ($1 < m < n$), non-coherent JT ($m = n$), and DPB ($m = 1$).

Remark 7: Non-coherent JT with $n = 2$ and DPB with $n = 3$ have similar performance in terms of M_1 and the meta distribution, as shown in Fig. 4(a) and Fig. 7.

Remark 8: The combined JT-DPB scheme provides a tradeoff between JT and DPB. For a given n, its performance and cost are in between JT and DPB.

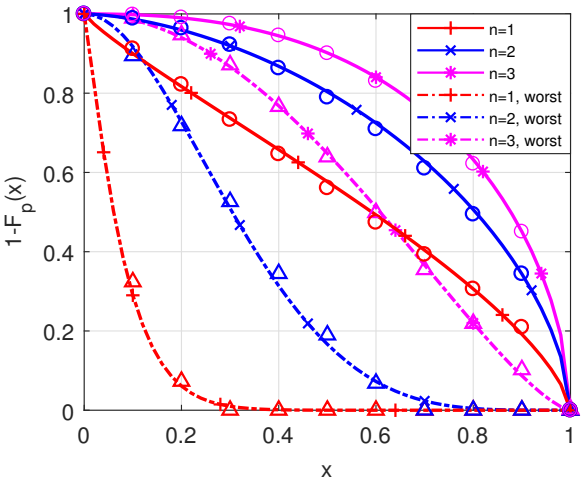

(a) non-coherent JT

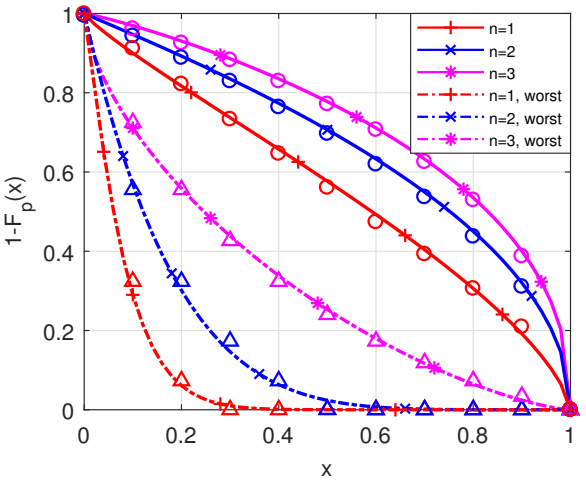

(b) DPB

Fig. 6. Exact meta distribution, its beta distribution approximation, and simulated results where $n = 1, 2, 3$, $\alpha = 4$, and $\theta = 0$ dB. The curves are the beta distribution approximation, the round markers are the simulated results, and the triangle markers are the exact meta distribution from (28).

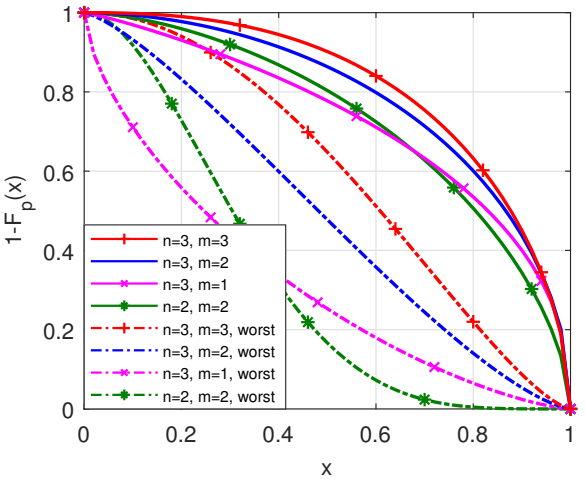

Fig. 7. Comparison of the beta distribution approximation of the meta distribution for non-coherent JT ($m = n$), DPB ($m = 1$), and the combined scheme JT-DPB ($1 < m < n$), where $\alpha = 4$, and $\theta = 0$ dB.

IV. Meta Distribution for DPS/DPB

A. SIR Model

In this section, we study the downlink DPS/DPB scheme, which is a combination of DPS and DPB. In this scheme, there is only one serving BS in the cooperation set, i.e., the size of set $\mathcal{O}$ is $m = 1$. We again consider two types of users—the general user and the worst-case user.

For DPS/DPB, the user receives a message that is transmitted by the BS with the best instantaneous channel condition

in the cooperation set, and the other BSs in the cooperation set are silenced. The serving BS for a certain user is determined by not only the normalized path loss (transmit power and distance) but also the fading. Hence the serving BS is chosen dynamically, and the desired signal is instantaneously the best, which is denoted by $S_{\mathrm{g}} = \max\limits_{i=1,\ldots,n} |h_{x_i}|^2 \gamma_i^{-1}$ and $S_{\mathrm{w}} = \max\limits_{i=1,\ldots,n} |h_{x_i}|^2 D^{-\alpha}$ for the general user and the worst-case user, respectively.

Similar to JT-DPB, the SIR of the general user with DPS/DPB is given by

$$\mathrm{SIR}_{\mathrm{g}}^{\mathrm{DPS/DPB}} = \frac{\max\limits_{i=1,\ldots,n} |h_{x_i}|^2 \gamma_i^{-1}}{\sum\limits_{i=n+1}^{\infty} \gamma_i^{-1} g_i}, \tag{32}$$

and the SIR of the worst-case user with DPS/DPB for $n = 1, 2, 3$ is given by

$$\begin{aligned}\mathrm{SIR}_{\mathrm{w}}^{\mathrm{DPS/DPB}} &= \frac{\max\limits_{i=1,\ldots,n} |h_{x_i}|^2 D^{-\alpha}}{\sum\limits_{i=n+1}^{\infty} \|x_i\|^{-\alpha} g_i} \\ &= \frac{\max\limits_{i=1,\ldots,n} |h_{x_i}|^2 D^{-\alpha}}{\sum\limits_{i=n+1}^{3} D^{-\alpha} g_i + \sum\limits_{i=4}^{\infty} \|x_i\|^{-\alpha} g_i}. \end{aligned} \tag{33}$$

B. Moments

Lemma 3 (Conditional success probability for the general user with DPS/DPB) *The conditional success probability for the general user with DPS/DPB is given by*

$$P_{\mathrm{s}}(\theta) = \sum_{k=1}^{n} (-1)^{k+1} \sum_{\gamma_1', \ldots, \gamma_k' \in \boldsymbol{\gamma}}^{\neq} p_n\big(\gamma_1' + \cdots + \gamma_k'\big), \tag{34}$$

where $\boldsymbol{\gamma} = \{\gamma_1, \ldots, \gamma_n\}$, and the notation "$\neq$" above the sum means $\gamma_i' \neq \gamma_j'$, $\forall i \neq j$, and

$$p_n(x) = \prod_{i=n+1}^{\infty} \frac{1}{1 + \frac{\theta}{x^{-1}\gamma_i^{-1}}}.$$

Proof: The conditional success probability can be expressed as

$$\begin{aligned} P_{\mathrm{s}}(\theta) &= \mathbb{P}\big(\mathrm{SIR}_{\mathrm{g}}^{\mathrm{DPS/DPB}} > \theta \mid \Xi\big) \\ &= \mathbb{P}\Big(\max_{i=1,\ldots,n} |h_{x_i}|^2 \gamma_i^{-1} > \theta I \mid \Xi\Big), \end{aligned} \tag{35}$$

which is the CCDF of the extreme value of random variables $|h_{x_i}|^2 \gamma_i^{-1}$ given the point process Ξ, where $I = \sum_{k=n+1}^{\infty} \gamma_k^{-1} g_k$.

The CDF of $Y \triangleq \max\limits_{i=1,\ldots,n} |h_{x_i}|^2 \gamma_i^{-1}$ can be derived as

$$\begin{aligned} &\mathbb{P}\big(Y \leq y \mid \Xi\big) \\ &= \mathbb{P}\big(|h_{x_1}|^2 \gamma_1^{-1} \leq y, |h_{x_2}|^2 \gamma_2^{-1} \leq y, \ldots, |h_{x_n}|^2 \gamma_n^{-1} \leq y \mid \Xi\big) \\ &\overset{(a)}{=} \prod_{i=1}^{n} \mathbb{P}\Big(|h_{x_i}|^2 \leq \frac{y}{\gamma_i^{-1}} \mid \Xi\Big), \end{aligned} \tag{36}$$

where (a) follows since $|h_{x_i}|^2$ are i.i.d. Hence (35) can be re-written as

$$\begin{aligned} P_{\mathrm{s}}(\theta) &= \mathbb{P}\big(Y > \theta I \mid \Xi\big) \\ &= 1 - \prod_{i=1}^{n} \mathbb{P}\Big(|h_{x_i}|^2 \leq \frac{\theta I}{\gamma_i^{-1}} \mid \Xi\Big) \\ &= \mathbb{E}\Big(1 - \prod_{i=1}^{n} \Big(1 - \exp\Big(-\frac{\theta I}{\gamma_i^{-1}}\Big)\Big) \mid \Xi\Big) \\ &= 1 - \mathbb{E}\Big(\underbrace{\prod_{i=1}^{n} \Big(1 - \prod_{k=n+1}^{\infty} \exp\Big(-\frac{\theta \gamma_k^{-1} g_k}{\gamma_i^{-1}}\Big)\Big)}_{A} \mid \Xi\Big). \end{aligned} \tag{37}$$

Letting $a_i = \prod_{k=n+1}^{\infty} \exp\big(-\frac{\theta \gamma_k^{-1} g_k}{\gamma_i^{-1}}\big)$, the product term A in (37) can be expanded as

$$A = \prod_{i=1}^{n} (1 - a_i) = 1 + \sum_{k=1}^{n} (-1)^k \sum_{a_1', \ldots, a_k' \in \boldsymbol{a}}^{\neq} a_1' a_2' \cdots a_k',$$

where $\boldsymbol{a} = \{a_1, a_2, \ldots, a_n\}$, then (37) can be expressed as

$$\begin{aligned} P_{\mathrm{s}}(\theta) &= 1 - \mathbb{E}\Big(\prod_{i=1}^{n} (1 - a_i) \mid \Xi\Big) \\ &= 1 - \mathbb{E}\Big(1 + \sum_{k=1}^{n} (-1)^k \sum_{a_1', \ldots, a_k' \in \boldsymbol{a}}^{\neq} a_1' a_2' \cdots a_k' \mid \Xi\Big) \\ &= \sum_{k=1}^{n} (-1)^{k+1} \underbrace{\sum_{a_1', \ldots, a_k' \in \boldsymbol{a}}^{\neq} \mathbb{E}\left(a_1' a_2' \cdots a_k' \mid \Xi\right)}_{B}. \end{aligned} \tag{38}$$

The term B in (38) can be expressed as

$$\begin{aligned} B &= \sum_{a_1', \ldots, a_k' \in \boldsymbol{a}}^{\neq} \mathbb{E}(a_1' a_2' \cdots a_k' \mid \Xi) \\ &= \sum_{\gamma_1', \ldots, \gamma_k' \in \boldsymbol{\gamma}}^{\neq} \mathbb{E}\Big(\prod_{i=n+1}^{\infty} \exp\Big(-\frac{\theta \gamma_i^{-1} g_i}{\gamma_1'^{-1}}\Big) \\ &\cdot \prod_{i=n+1}^{\infty} \exp\Big(-\frac{\theta \gamma_i^{-1} g_i}{\gamma_2'^{-1}}\Big) \cdots \prod_{i=n+1}^{\infty} \exp\Big(-\frac{\theta \gamma_i^{-1} g_i}{\gamma_k'^{-1}}\Big) \mid \Xi\Big) \\ &= \sum_{\gamma_1', \ldots, \gamma_k' \in \boldsymbol{\gamma}}^{\neq} \mathbb{E}\Big(\prod_{i=n+1}^{\infty} \exp\Big(\frac{-\theta \gamma_i^{-1} g_i}{(\gamma_1' + \gamma_2' + \cdots + \gamma_k')^{-1}}\Big) \mid \Xi\Big) \\ &\overset{(a)}{=} \sum_{\gamma_1', \ldots, \gamma_k' \in \boldsymbol{\gamma}}^{\neq} \prod_{i=n+1}^{\infty} \frac{1}{1 + \frac{\theta}{(\gamma_1' + \gamma_2' + \cdots + \gamma_k')^{-1}} \gamma_i^{-1}}, \end{aligned}$$

where $\boldsymbol{\gamma} = \{\gamma_1, \ldots, \gamma_n\}$, and (a) follows since $g_k = |h_{x_k}|^2$ is exponentially distributed with unit mean. The final result in (34) is obtained after some simplification. ∎

Theorem 3 (First Moment of $P_{\mathrm{s}}(\theta)$ for the general user with DPS/DPB) *The first moment M_1 of the conditional success probability $P_{\mathrm{s}}(\theta)$, i.e., the standard success proba-*

bility, for the general user in downlink cellular networks with DPS/DPB is given by

$$M_1 = \sum_{k=1}^{n} (-1)^{k+1} \sum_{u'_1,\ldots,u'_k \in \mathbf{u}}^{\neq} m_n\Big({u'_1}^{1/\delta} + \cdots + {u'_k}^{1/\delta}\Big), \tag{39}$$

where $\mathbf{u} = \{u_1, \ldots, u_n\}$*, and*

$$m_n(x) = \int\limits_{\substack{0<u_1<\cdots \\ \cdots<u_n<\infty}} \exp\bigg(- u_n \ {}_2F_1\Big(1, -\delta; 1-\delta; \frac{-\theta}{u_n^{1/\delta}/x}\Big)\bigg) \mathrm{d}\mathbf{u}.$$

Proof: In accordance with Lemma 3, M_1 follows as

$$\begin{aligned} M_1 &= \mathbb{E}(P_{\mathrm{s}}(\theta)) \\ &= \mathbb{E}\bigg(\sum_{k=1}^{n} (-1)^{k+1} \sum_{\gamma'_1,\ldots,\gamma'_k \in \boldsymbol{\gamma}}^{\neq} p_n\big(\gamma'_1 + \cdots + \gamma'_k\big)\bigg) \\ &= \sum_{k=1}^{n} (-1)^{k+1} \sum_{\gamma'_1,\ldots,\gamma'_k \in \boldsymbol{\gamma}}^{\neq} \mathbb{E}\big(p_n\big(\gamma'_1 + \cdots + \gamma'_k\big)\big). \end{aligned} \tag{40}$$

The term $\mathbb{E}\left(p_n\left(\gamma_x\right)\right)$ is similar with (14) in the proof of Theorem 1, and can be expressed as

$$\begin{aligned} &\mathbb{E}(p_n(\gamma_x)) = \mathbb{E}\bigg(\prod_{i=n+1}^{\infty} \frac{1}{1 + \frac{\theta}{\gamma_x^{-1}\gamma_i^{-1}}}\bigg) \\ &\overset{(a)}{=} \int\limits_{\substack{0<r_1<\cdots \\ \cdots<r_n<\infty}} \exp\bigg(- \int_{r_n}^{\infty} \Big(1 - \frac{1}{1 + \frac{\theta}{r_x^{-1} t^{-1}}}\Big) \lambda(t)\mathrm{d}t\bigg) f_{\boldsymbol{\gamma}}(\boldsymbol{r})\mathrm{d}\boldsymbol{r} \\ &\overset{(b)}{=} \int\limits_{\substack{0<r_1<\cdots \\ \cdots<r_n<\infty}} (\delta q)^n \prod_{i=1}^{n} r_i^{\delta-1} \\ &\qquad \cdot \exp\bigg(-q r_n^{\delta} \ {}_2F_1\Big(1, -\delta; 1-\delta; \frac{-\theta}{r_n r_x^{-1}}\Big)\bigg) \mathrm{d}\boldsymbol{r}, \end{aligned} \tag{41}$$

where (a) follows from the PGFL of the non-homogeneous PPP Ξ; $f_{\boldsymbol{\gamma}}(\boldsymbol{r})$ is the PDF of $\boldsymbol{\gamma}$ given in (13); $\lambda(t)$ is the intensity of the non-homogeneous PPP Ξ given in (8); (b) is derived by using the Gaussian hypergeometric function ${}_2F_1(\cdot)$ and $q = \pi \sum_{i=1}^{K} \lambda_i P_i^{\delta}$.

By substituting (41) into (40) and changing the integral variable $u_i = q r_i^{\delta}$, the result in (39) is obtained after some simplification. ∎

Lemma 4 (Conditional success probability for the worst–case user with DPS/DPB) *For $n = 1, 2, 3$, the conditional success probability for the worst-case user with DPS/DPB is given by*

$$P_{\mathrm{s}}(\theta) = \sum_{k=1}^{n} \binom{n}{k} (-1)^{k+1} (1 + k\theta)^{n-3} \prod_{i=4}^{\infty} \frac{1}{1 + k\frac{\theta \|x_i\|^{-\alpha}}{D^{-\alpha}}}. \tag{42}$$

Proof: Similar to (36), the CDF of $Y \triangleq \max\limits_{i=1,\ldots,n} D^{-\alpha} |h_{x_i}|^2$ can be expressed as

$$\mathbb{P}(Y \le y \mid \Phi) = \prod_{i=1}^{n} \mathbb{P}\Big(|h_{x_i}|^2 \le \frac{y}{D^{-\alpha}} \mid \Phi\Big).$$

Then the conditional success probability can be derived as

$$\begin{aligned} P_{\mathrm{s}}(\theta) &= \mathbb{P}(Y > \theta I \mid \Phi) = 1 - \prod_{i=1}^{n} \mathbb{P}\Big(|h_{x_i}|^2 \le \frac{\theta I}{D^{-\alpha}} \mid \Phi\Big) \\ &\overset{(a)}{=} \mathbb{E}\bigg(1 - \Big(1 - \exp\Big(-\frac{\theta I}{D^{-\alpha}}\Big)\Big)^n \mid \Phi\bigg) \\ &= 1 - \mathbb{E}\bigg(\Big(1 - \prod_{i=n+1}^{3} \exp\left(-\theta g_i\right) \\ &\qquad \cdot \prod_{i=4}^{\infty} \exp\bigg(- \frac{\theta \|x_i\|^{-\alpha}}{D^{-\alpha}} g_i\bigg)\Big)^n \mid \Phi\bigg) \\ &\overset{(b)}{=} 1 - \mathbb{E}\bigg(\sum_{k=0}^{n} \binom{n}{k} (-1)^k \prod_{i=n+1}^{3} \exp\left(-k\theta g_i\right) \\ &\qquad \cdot \prod_{i=4}^{\infty} \exp\bigg(- k\frac{\theta \|x_i\|^{-\alpha}}{D^{-\alpha}} g_i\bigg) \mid \Phi\bigg) \\ &\overset{(c)}{=} 1 + \sum_{k=0}^{n} \binom{n}{k} (-1)^{k+1} \bigg(\frac{1}{1+k\theta}\bigg)^{3-n} \prod_{i=4}^{\infty} \frac{1}{1 + k\frac{\theta\|x_i\|^{-\alpha}}{D^{-\alpha}}}, \end{aligned}$$

where (a) follows since $|h_{x_i}|^2$ is independently exponentially distributed with unit mean; (b) follows from the binomial theorem $(a+b)^n \equiv \sum_{k=0}^{n} \binom{n}{k} a^{n-k} b^k$; and (c) follows since $g_i = |h_{x_i}|^2$ is independently exponentially distributed with unit mean. After some simplification the result in (42) is obtained. ∎

Theorem 4 (First and second moments of $P_{\mathrm{s}}(\theta)$ for the worst-case user with DPS/DPB) *For $n = 1, 2, 3$, the first moment M_1 of the conditional success probability $P_{\mathrm{s}}(\theta)$, i.e., the standard success probability, for the worst-case user in downlink cellular networks with DPS/DPB is given by*

$$M_1 = \sum_{k=1}^{n} \binom{n}{k} (-1)^{k+1} \frac{\big(1+k\theta\big)^{n-3}}{\big({}_2F_1\big(1, -\delta; 1-\delta; -k\theta\big)\big)^2}, \tag{43}$$

and the second moment M_2 of $P_{\mathrm{s}}(\theta)$ is given by

$$M_2 = \begin{cases} \dfrac{F(\theta)}{(1+\theta)^4}, & n = 1 \\ \dfrac{4F(\theta)}{(1+\theta)^2} + \dfrac{F(2\theta)}{(1+2\theta)^2} - \dfrac{4Q(3\theta, 2\theta^2)}{(1+\theta)(1+2\theta)}, & n = 2 \\ 9F(\theta) + 9F(2\theta) + F(3\theta) - 18Q(3\theta, 2\theta^2) \\ \qquad + 6Q(4\theta, 3\theta^2) - 6Q(5\theta, 6\theta^2), & n = 3, \end{cases} \tag{44}$$

where

$$F(x) \triangleq \left({}_2F_1(2, -\delta; 1-\delta; -x)\right)^{-2},$$

$$Q(u,v) \triangleq \int_0^{\infty} \exp\bigg(- \int_r^{\infty} 2\pi\lambda x \cdot \bigg(1 - \frac{1}{1 + ur^{\alpha}x^{-\alpha} + vr^{2\alpha}x^{-2\alpha}}\bigg) \mathrm{d}x\bigg) f_D(r)\mathrm{d}r.$$

Proof: We first express the first moment of $P_{\rm s}(\theta)$ as

$$M_1 = \mathbb{E}(P_{\rm s}(\theta)) = \sum_{k=1}^{n} \binom{n}{k} (-1)^{k+1} \underbrace{(1+k\theta)^{n-3}\, \mathbb{E}\left(\prod_{i=4}^{\infty} \frac{1}{1+k\frac{\theta\|x_i\|^{-\alpha}}{D^{-\alpha}}} \right)}_{A}. \tag{45}$$

We notice that the term A in (45) has almost the same form as the expression in the proof of Theorem 2. Similarly, we can get the results in (43).

Then for M_2, we take $n = 2$ as an example, and the derivation of M_2 with $n = 1, 3$ is similar.

When $n = 2$, the conditional success probability $P_{\rm s}(\theta)$ in (42) can be expressed as

$$P_{\rm s}(\theta) = \frac{2}{1+\theta} \prod_{i=4}^{\infty} \frac{1}{1+\frac{\theta\|x_i\|^{-\alpha}}{D^{-\alpha}}} - \frac{1}{1+2\theta} \prod_{i=4}^{\infty} \frac{1}{1+2\frac{\theta\|x_i\|^{-\alpha}}{D^{-\alpha}}},$$

and we obtain M_2 in the form

$$\begin{aligned} M_2 &= \mathbb{E}(P_{\rm s}(\theta)^2) \\ &= \frac{4}{(1+\theta)^2} \mathbb{E}\left(\prod_{i=4}^{\infty} \frac{1}{\left(1+\frac{\theta\|x_i\|^{-\alpha}}{D^{-\alpha}}\right)^2} \right) \\ &\quad + \frac{1}{(1+2\theta)^2} \mathbb{E}\left(\prod_{i=4}^{\infty} \frac{1}{\left(1+2\frac{\theta\|x_i\|^{-\alpha}}{D^{-\alpha}}\right)^2} \right) \\ &\quad - \frac{4}{(1+\theta)(1+2\theta)} \mathbb{E}\left(\prod_{i=4}^{\infty} \frac{1}{1+3\frac{\theta\|x_i\|^{-\alpha}}{D^{-\alpha}} + 2\frac{\theta^2\|x_i\|^{-2\alpha}}{D^{-2\alpha}}} \right) \\ &= \frac{4}{(1+\theta)^2} \left({}_2F_1\left(2, -\delta; 1-\delta; -\theta\right)\right)^{-2} \\ &\quad + \frac{1}{(1+2\theta)^2} \left({}_2F_1\left(2, -\delta; 1-\delta; -2\theta\right)\right)^{-2} \\ &\quad - \frac{4}{(1+\theta)(1+2\theta)} \int_0^{\infty} \exp\left(-\int_r^{\infty} 2\pi\lambda x \right. \\ &\quad \left. \cdot \left(1 - \frac{1}{1+3\theta r^{\alpha} x^{-\alpha} + 2\theta^2 r^{2\alpha} x^{-2\alpha}}\right) {\rm d}x \right) f_D(r) {\rm d}r, \end{aligned}$$

where $f_D(r)$ is given in (21). After some simplification (44) is obtained. ∎

The standard success probability $p_{\rm s} \equiv M_1$ and the variance of the conditional success probability are shown in Fig. 8.

C. Meta Distribution and its Beta Approximation

We follow the same analysis methods as for JT-DPB. Since the SIR distribution only depends on the intensity function $\lambda(x)$ in (8), we again conclude that the meta distribution for DPS/DPB is independent of the number of network tiers and their respective densities and transmit powers. Hence, for the convenience of comparison, the simulation setups in this section are the same as in Sec. III.

For DPS/DPB, Fig. 9 shows the beta approximation for the worst-case user and the simulation results for both general and worst-case users. Due to the complexity of the higher-order moments in this scheme, the beta approximation for the general user is too unwieldy to gain direct insight, let alone the exact meta distribution for both types of users. As shown in Fig. 9, for the worst-case user with DPS/DPB, the accuracy

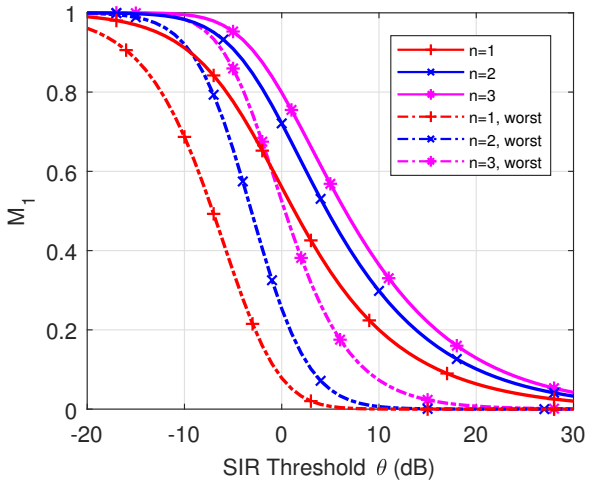

(a) M_1

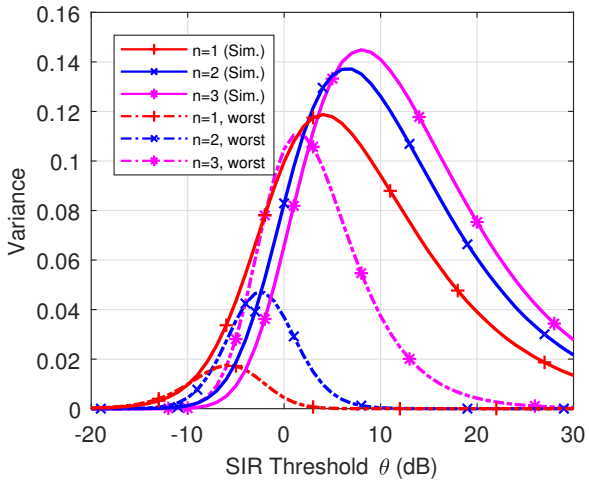

(b) Variance $M_2 - M_1^2$

Fig. 8. M_1 and the variance (i.e. $M_2 - M_1^2$) of $P_{\rm s}(\theta)$ for DPS/DPB where $n = 1, 2, 3$, and $\alpha = 4$. The variance for the general user is obtained by simulation.

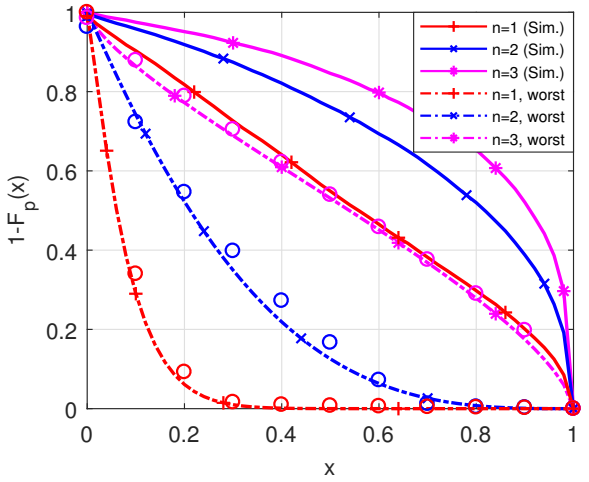

Fig. 9. Beta distribution approximation and simulation result for DPS/DPB where $n = 1, 2, 3$, $\alpha = 4$, and $\theta = 0$ dB. The dashed curves are the beta distribution approximation, and the solid curves and the round markers are the simulated results.

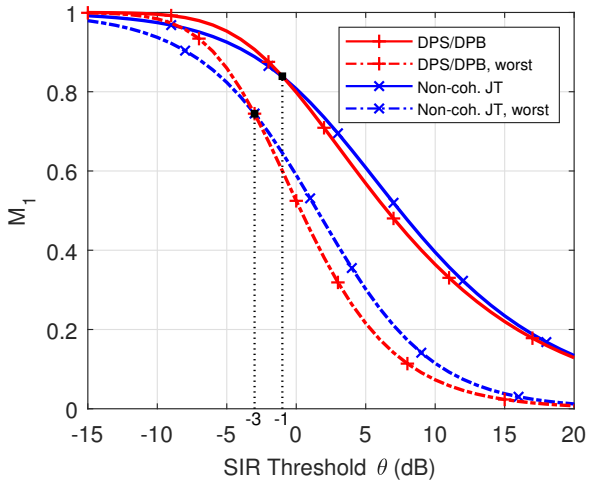

(a) M_1

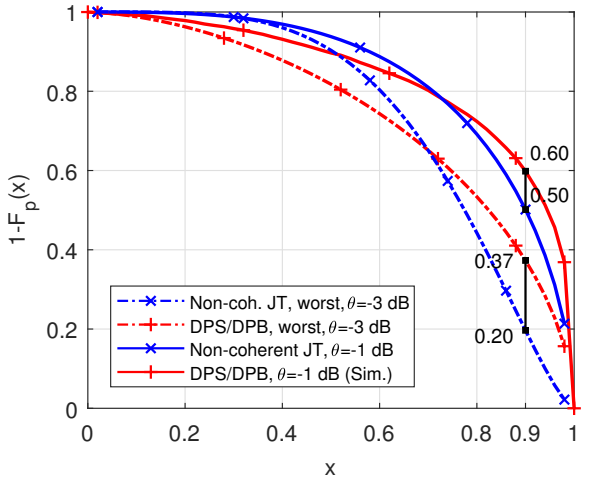

(b) Meta distribution

Fig. 10. M_1 and meta distribution of the general user and the worst-case user with DPS/DPB or non-coherent JT, where $n = 3$, and $\alpha = 4$.

of the beta distribution approximation is also confirmed by comparing the approximations with simulation results.

V. Insights and Importance of the Meta Distribution for CoMP Networks

In Fig. 6 and Fig. 9, the accuracy of the beta approximation for meta distribution is confirmed. Hence, in this section, we use the beta approximation to compare and discuss our results.

A. Conditional Link Reliability

The meta distribution provides more fine-grained information for the individual links than the standard success probability. For example, Fig. 10 shows the standard success probability M_1 and the meta distribution $\bar{F}_{P_s}$ of the general user and the worst-case user with DPS/DPB or non-coherent JT where $n = 3$, and $\alpha = 4$. In Fig. 10(a), it is observed that, for the general user with non-coherent JT or DPS/DPB, $M_{1,\,\text{DPS/DPB}} \approx M_{1,\,\text{JT}}$ for $\theta = -1$ dB, and the standard success probability does not provide more information to distinguish these two schemes. However, the meta distribution shows more fine-grained information. As shown in Fig. 10(b), the meta distribution $\bar{F}_{P_s}$ for non-coherent JT and DPS/DPB is different. There are 60% users in a non-coherent JT network achieving 90% link reliability for $\theta = -1$ dB, but 50% users in a DPS/DPB network. Hence, although M_1 is approximately equal, DPS/DPB has more highly reliable links than non-coherent JT. The difference is even more prominent for the worst-case user when $\theta = -3$ dB.

B. Comparison of the Different CoMP Schemes

In the prior sections, we studied non-coherent JT, DPB, and DPS/DPB by analysis, where the non-coherent JT is without precoder. Among these different CoMP schemes, the interference is the same in all schemes for a given n, and the only difference is the combining modes of the desired signals, which are given by

$$S = \begin{cases} \left|h_{x_1}\right|^2 \gamma_1^{-1}, & \text{DPB only or Non-CoMP} \\ \max\limits_{i=1,\ldots,n} \left|h_{x_i}\right|^2 \gamma_i^{-1}, & \text{DPS/DPB} \\ \left|\sum\limits_{k=1}^{n} h_{x_k} \gamma_k^{-1/2}\right|^2, & \text{Non-coherent JT} \\ \left(\sum\limits_{k=1}^{n} \left|h_{x_k}\right| \gamma_k^{-1/2}\right)^2, & \text{Coherent JT.} \end{cases} \tag{46}$$

Here we also simulate the coherent JT and the enhanced non-coherent JT which uses individual precoders, i.e., $S = \sum_{k=1}^{n} \left|h_{x_k}\right|^2 \gamma_k^{-1}$, and compare these results as shown in Fig. 11 and Fig. 12.

Fig. 12 shows that all these CoMP schemes benefit the worst-case user more than the general user, which verifies the intuition that CoMP can significantly improve the system performance and, especially, enhance the cell-edge coverage. Fig. 12 also shows that the worst-case user with DPS/DPB ($n = 3$) can achieve the similar performance compared with the general user without cooperation.

Qualitatively, it is observed from Fig. 11 and Fig. 12 that most of the results are consistent with our intuition of CoMP, with the exception that the non-coherent JT scheme in Section III does not provide more gain than the DPS/DPB in Section IV. We analyze this phenomenon using the combining modes of the desired signals given in (46). The performance gain of JT is closely related to the combining mode of the desired signals. It is easily seen that $\left|h_{x_1}\right|^2 \gamma_1^{-1} \leq \max\limits_{i=1,\ldots,n} \left|h_{x_i}\right|^2 \gamma_i^{-1} \leq \sum_{k=1}^{n} \left|h_{x_k}\right|^2 \gamma_k^{-1} \leq \left(\sum_{k=1}^{n} \left|h_{x_k}\right| \gamma_k^{-1/2}\right)^2$, and $\left|h_{x_1}\right|^2 \gamma_1^{-1} \leq \left|\sum_{k=1}^{n} h_{x_k} \gamma_k^{-1/2}\right|^2 \leq \sum_{k=1}^{n} \left|h_{x_k}\right|^2 \gamma_k^{-1}$. For non-coherent JT without precoder, blind demodulation is used at the receiver side. Since it can not exploit the diversity gain of JT, non-coherent JT does not provide a significant gain compared with DPS/DPB. However, for enhanced non-coherent JT, because of the individual precoding, the performance of this scheme is better. For coherent JT, the diversity gain of JT can be fully harvested because of the joint precoding, hence the performance of coherent JT is significantly higher than DPS/DPB.

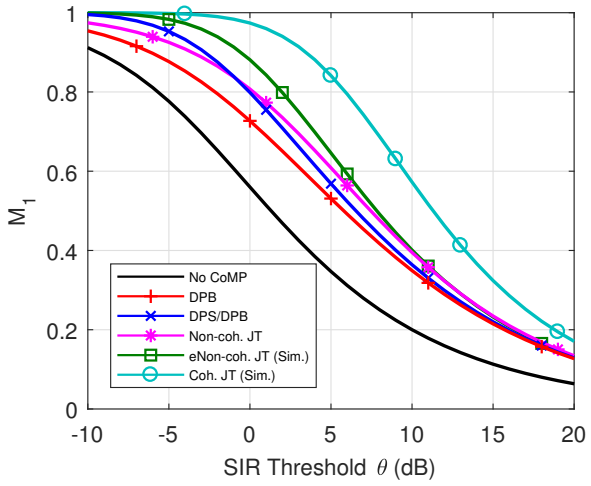

(a) M_1

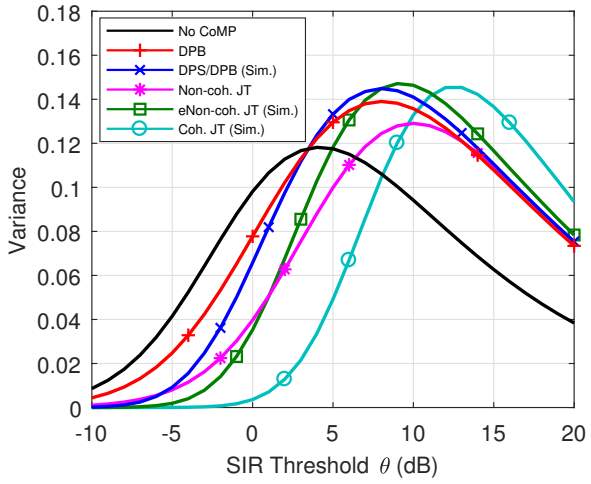

(b) Variance $M_2 - M_1^2$

Fig. 11. Comparison of M_1 and the variance (i.e. $M_2 - M_1^2$) of $P_{\rm s}(\theta)$ for the general user with DPB, DPS/DPB, and three JT schemes, where $n = 3$, and $\alpha = 4$. The variance for DPS/DPB, and the curves for non-coherent JT and coherent JT are obtained by simulation.

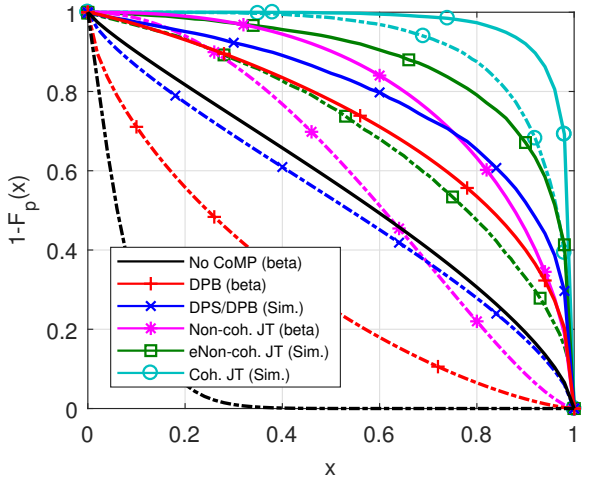

Fig. 12. Comparison of the beta approximation or the simulated meta distribution for the general user and the worst-case user with DPB, DPS/DPB, and three JT schemes, where $n = 3$, $\alpha = 4$, and $\theta = 0$ dB. The dashed lines correspond to the worst-case user. The curve for the worst-case user with DPS/DPB is obtained by beta approximation.

The performance of non-coherent JT without precoder can be regarded as a lower bound for the performance of other JT schemes.

C. The Size of the Cooperation Set

As we can see from the figures in this paper, for the general user with all these CoMP schemes, the gain from $n = 1$ to $n = 2$ is larger than the gain from $n = 2$ to $n = 3$. For example, as shown in Fig. 6(a), when the reliability value $x = 0.6$, for the general user with non-coherent JT, the gain of meta distribution from $n = 1$ to $n = 2$ is about 45%, while the gain from $n = 2$ to $n = 3$ is about 16%. In contrast, for the worst-case user, this is not the case, since the distances from the serving user to the nearest three BSs are equal. In short, the performance gain associated with CoMP decreases as the size of the cooperation set increases. Hence, given the overhead associated with CoMP, there exists an optimum size of the cooperation set.

VI. Conclusion

This paper studies the meta distribution in downlink Poisson cellular networks with multiple types of CoMP schemes including JT, DPB, and DPS/DPB. We give a general scheme for JT-DPB with JT and DPB as special cases. For each CoMP scheme, we consider two types of users—the general user and the worst-case user. The b-th moment of conditional success probability is derived for both types of users with JT-DPB. For DPS/DPB, the first moment (standard success probability) for the general user and the first and second moments for the worst-case user are derived. We calculate the exact meta distribution for the worst-case user with JT-DPB and calculate the beta distribution approximation of the exact meta distribution for almost all schemes and user types. We show that the beta approximation provides a great match for the exact meta distribution.

The mean local delay is also derived for both types of users with JT-DPB, and the analysis shows that for both the general and worst-case users, the critical value of the SIR threshold for finite mean local delay with non-coherent JT is $(1/\delta - 1)n$, while with DPB it is $1/\delta - 1$.

By the comparison and analysis of the meta distribution of DPB, DPS/DPB, and JT, we provide more fine-grained information on the link reliability for different CoMP schemes. The analysis shows: 1) CoMP can significantly improve the system performance and, especially, enhance the cell-edge coverage, 2) the performance gain of JT is closely related to the combining mode, and 3) the performance gain associated with CoMP decreases as the size of the cooperation set increases.

Based on the study in this paper, the future work includes: 1) considering the spatial correlation by modeling the networks by more general point processes, e.g., determinantal point processes such as the Ginibre process [34], [35]; 2) analyzing the effect of incomplete/imperfect CSI; 3) extending to more scenarios, such as MIMO or relaying.

REFERENCES

[1] Cisco, *Cisco Visual Networking Index: Global Mobile Data Traffic Forecast Update, 2016-2021*, Cisco white paper, Feb. 2017, Available at http://www.cisco.com/c/en/us/solutions/collateral/service-provider/visual-networking-index-vni/mobile-white-paper-c11-520862.html.

[2] H. ElSawy, A. Sultan-Salem, M.-S. Alouini, and M. Z. Win, "Modeling and analysis of cellular networks using stochastic geometry: A tutorial," *IEEE Commun. Surv. Tutorials*, vol. 19, pp. 167–203, Firstquarter 2016.

[3] M. Haenggi, "The meta distribution of the SIR in Poisson bipolar and cellular networks," *IEEE Trans. Wireless Commun.*, vol. 15, pp. 2577–2589, Apr. 2016.

[4] J. Gil-Pelaez, "Note on the inversion theorem," *Biometrika*, vol. 38, pp. 481–482, Dec. 1951.

[5] M. Haenggi, *Stochastic Geometry for Wireless Networks*. Cambridge University Press, 2012.

[6] M. Haenggi, J. G. Andrews, F. Baccelli, O. Dousse, and M. Franceschetti, "Stochastic geometry and random graphs for the analysis and design of wireless networks," *IEEE J. Sel. Areas Commun.*, vol. 27, pp. 1029–1046, Sep. 2009.

[7] J. G. Andrews, F. Baccelli, and R. K. Ganti, "A tractable approach to coverage and rate in cellular networks," *IEEE Trans. Commun.*, vol. 59, pp. 3122–3134, Nov. 2011.

[8] H. S. Dhillon, R. K. Ganti, F. Baccelli, and J. G. Andrews, "Modeling and analysis of K-tier downlink heterogeneous cellular networks," *IEEE J. Sel. Areas Commun.*, vol. 30, pp. 550–560, Apr. 2012.

[9] X. Zhang and M. Haenggi, "A stochastic geometry analysis of inter-cell interference coordination and intra-cell diversity," *IEEE Trans. Wireless Commun.*, vol. 13, pp. 6655–6669, Dec. 2014.

[10] M. Salehi, A. Mohammadi, and M. Haenggi, "Analysis of D2D underlaid cellular networks: SIR meta distribution and mean local delay," *IEEE Trans. Commun.*, vol. 65, pp. 2904–2916, Jul. 2017.

[11] Y. Wang, M. Haenggi, and Z. Tan, "The meta distribution of the SIR for cellular networks with power control," Submitted. Available at http://arxiv.org/pdf/1702.01864v1.

[12] N. Deng and M. Haenggi, "A fine-grained analysis of millimeter-wave device-to-device networks," *IEEE Trans. Commun.*, 2017, to appear.

[13] 3GPP, "Coordinated multi-point operation for LTE physical layer aspects," TR 36.819, Tech. Rep., Sep. 2011, available at http://www.3gpp.org/DynaReport/36819.htm.

[14] Q. Cui, H. Song, H. Wang, M. Valkama, and A. A. Dowhuszko, "Capacity analysis of joint transmission CoMP with adaptive modulation," *IEEE Trans. Veh. Technol.*, vol. 66, pp. 1876–1881, 2017.

[15] G. Nigam, P. Minero, and M. Haenggi, "Coordinated multipoint joint transmission in heterogeneous networks," *IEEE Trans. Commun.*, vol. 62, pp. 4134–4146, Nov. 2014.

[16] ——, "Spatiotemporal cooperation in heterogeneous cellular networks," *IEEE J. Sel. Areas Commun.*, vol. 33, pp. 1253–1265, Jun. 2015.

[17] G. Nigam and P. Minero, "Spatiotemporal base station cooperation in a cellular network: The worst-case user," in *Proc. IEEE GLOBECOM*, Dec. 2015, pp. 1–6.

[18] R. Tanbourgi, S. Singh, J. G. Andrews, and F. K. Jondral, "A tractable model for noncoherent joint-transmission base station cooperation," *IEEE Trans. Wireless Commun.*, vol. 13, pp. 4959–4973, Sep. 2014.

[19] W. Zuo, H. Xia, and C. Feng, "A novel coordinated multi-point transmission in dense small cell deployment," in *Proc. 2015 IEEE 26th Annual International Symposium on Personal, Indoor, and Mobile Radio Communications (PIMRC)*. IEEE, 2015, pp. 1872–1877.

[20] Y.-N. R. Li, J. Li, W. Li, Y. Xue, and H. Wu, "CoMP and interference coordination in heterogeneous network for LTE-advanced," in *Proc. IEEE GLOBECOM Workshops*. IEEE, 2012, pp. 1107–1111.

[21] D. Marabissi, G. Bartoli, R. Fantacci, and M. Pucci, "An optimized CoMP transmission for a heterogeneous network using eICIC approach," *IEEE Trans. Veh. Technol.*, vol. 65, pp. 8230–8239, 2016.

[22] Y. Liu, L. Lu, G. Y. Li, Q. Cui, and W. Han, "Joint user association and spectrum allocation for small cell networks with wireless backhauls," *IEEE Wireless Commun. Lett.*, vol. 5, pp. 496–499, Oct. 2016.

[23] Q. Cui, H. Wang, P. Hu, X. Tao, P. Zhang, J. Hamalainen, and L. Xia, "Evolution of limited-feedback CoMP systems from 4G to 5G: CoMP features and limited-feedback approaches," *IEEE Veh. Technol. Mag.*, vol. 9, pp. 94–103, Sep. 2014.

[24] H. Zhang, N. B. Mehta, A. F. Molisch, J. Zhang, and S. H. Dai, "Asynchronous interference mitigation in cooperative base station systems," *IEEE Trans. Wireless Commun.*, vol. 7, pp. 155–165, Jan. 2008.

[25] W. Hardjawana, B. Vucetic, and Y. Li, "Multi-user cooperative base station systems with joint precoding and beamforming," *IEEE J. Sel. Topics Signal Process.*, vol. 3, pp. 1079–1093, Dec. 2009.

[26] P. Marsch and G. P. Fettweis, *Coordinated Multi-point in Mobile Communications: from Theory to Practice*. Cambridge University Press, 2011.

[27] R. Apelfröjd and M. Sternad, "Design and measurement-based evaluations of coherent JT CoMP: a study of precoding, user grouping and resource allocation using predicted CSI," *EURASIP J. Wireless Commun. Netw.*, vol. 2014, pp. 1–20, 2014.

[28] J. Lee, Y. Kim, H. Lee, B. L. Ng, D. Mazzarese, J. Liu, W. Xiao, and Y. Zhou, "Coordinated multipoint transmission and reception in LTE-advanced systems," *IEEE Commun. Mag.*, vol. 50, pp. 44–50, Nov. 2012.

[29] E. Dahlman, S. Parkvall, and J. Skold, *4G: LTE/LTE-Advanced for Mobile Broadband*, 2nd ed. Academic Press, 2013.

[30] T. R. Lakshmana, B. Makki, and T. Svensson, "Frequency allocation in non-coherent joint transmission CoMP networks," in *Proc. IEEE ICC Workshops*, Jun. 2014, pp. 610–615.

[31] H. Wu, X. Tao, and N. Li, "Coverage analysis for k-tier heterogeneous networks with multi-cell cooperation," in *Proc. IEEE GLOBECOM Workshops*, Dec. 2015, pp. 1–5.

[32] M. Haenggi, "The local delay in Poisson networks," *IEEE Trans. Inf. Theory*, vol. 59, pp. 1788–1802, Mar. 2013.

[33] F. Baccelli, B. Błaszczyszyn, and M.-O. Haji-Mirsadeghi, "Optimal paths on the space-time SINR random graph," *Adv. Appl. Probab.*, vol. 43, pp. 131–150, 2011.

[34] N. Deng, W. Zhou, and M. Haenggi, "The Ginibre point process as a model for wireless networks with repulsion," *IEEE Trans. Wireless Commun.*, vol. 14, pp. 107–121, Jan. 2015.

[35] H.-B. Kong, P. Wang, D. Niyato, and Y. Cheng, "Modeling and analysis of wireless sensor networks with/without energy harvesting using Ginibre point processes," *IEEE Trans. Wireless Commun.*, vol. 16, pp. 3700–3713, Jun. 2017.